Available online at www.sciencedirect.com
SCIENCE DIRECT
Trans. Nonferrous Met. Soc. China 17(2007) 1230−1235
Transactions of Nonferrous Metals Society of China
www.csu.edu.cn/ysxb/

Microstructure and mechanical properties of laser melting deposited Ti_2Ni_3Si/NiTi Laves alloys

DONG Li-xin(董李欣), WANG Hua-ming(王华明)

Laboratory of Laser Materials Processing and Manufacturing, School of Materials Science and Engineering, Beihang University, Beijing 100083, China

Received 15 July 2007; accepted 10 September 2007

Abstract: Two Ti_2Ni_3Si/NiTi Laves phase alloys with chemical compositions of Ni-39Ti-11Si and Ni-42Ti-8Si (%, mole fraction, the same below), respectively, were fabricated by the laser melting deposition manufacturing process, aiming at studying the effect of Ti, Si contents on microstructure and mechanical properties of the alloys. The Ni-39Ti-11Si alloy consisting of Ti_2Ni_3Si primary dendrites and Ti_2Ni_3Si/NiTi eutectic matrix is a conventional hypereutectic Laves phase alloy while the Ni-42Ti-8Si alloy being made up of NiTi primary dendrites uniformly distributed in Ti_2Ni_3Si/NiTi eutectic is a new hypoeutectic alloy. Mechanical properties of the alloys were investigated by nano-indentation test. The results show that the decrease of Si and the increase of Ti contents change the microstructures of the alloys from hypereutectic to hypoeutectic, which influences the mechanical properties of the alloys remarkably. Corrosion behaviors of the alloys were also evaluated by potentiodynamic anodic polarization curves.

Key words: Ti_2Ni_3Si; NiTi; Laves phase alloy; laser melting deposition

1 Introduction

Intermetallic alloys based on Laves phase intermetallic compound, usually consisting of a hard Laves phase dispersed in a matrix of eutectic or relatively soft solid solution, are a new class of metallic materials that have many attractive properties such as high strength, resistance to wear and corrosion for industrial application[1−3]. The outstanding wear and corrosion properties of these alloys are usually dependent on the volume fraction of intermetallic Laves phase, most of which possess high hardness, high melting temperature and strong inter-atomic bonds. Although certain Laves phase alloys such as Co-based T-400, T-800 alloys, in which the intermetallic phase is a $MgZn_2$ type Laves phase, a close-packed hexagonal (hcp) compound of Co, Mo and Si as Co_3Mo_2Si or CoMoSi, are known for wide commercial use in wear and corrosion applications, the extensive use of these alloys is limited due to their extremely low ductility and fracture toughness, which also result from the large volume fraction of the brittle Laves phase intermetallic compound[4−7]. Accordingly, improvement of mechanical properties such as ductility and fracture toughness without losing their excellent wear and corrosion resistance is the most desirable for Laves phase alloys. The beneficial effects of additional toughening phases on ductility and toughness are demonstrated by the results of recent studies on in-suit Laves phase alloys fabricated by the laser melting deposition manufacturing process[8−10]. The intermetallic compound NiTi, well-known for its prominent shape memory effect, hyperelasticity and high ductility[11−12], is recognized and demonstrated to be an outstanding toughening phase. Furthermore, NiTi was reported to have not only fairly good wear resistance because of its superelasticity originating from the martensitic transformation and the preferred orientation of martensite[13−14], but also excellent corrosion resistance by virtue of the formation of a thin dense passive film[15−16]. With the topologically-closed-packed(TCP) hP12 $MgZn_2$ type crystal structure, Ti_2Ni_3Si is the optimal Laves phase intermetallic compound to be toughened by NiTi through

Foundation item: Project(50625413) supported by the National Natural Science Foundation of China
Corresponding author: DONG Li-xin; Tel: +86-10-82317102; Fax: +86-10-82338131; E-mail: joanskys@163.com

the in-suit laser melting deposition manufacturing process. Therefore, a multiphase Ti_2Ni_3Si-based alloy with the ductile NiTi as toughening phase was expected to be a new first-class Laves phase alloy having an outstanding combination of mechanical properties and wear as well as corrosion properties[17−18].

In this work, two Ti_2Ni_3Si/NiTi alloys were fabricated by the laser melting deposition manufacturing process. The effects of Ti, Si contents on microstructure and mechanical properties of the alloys were investigated and other properties, such as corrosion behavior of the alloys, were also evaluated.

2 Experimental

In order to investigate the influence of Ti, Si contents on microstructure, mechanical properties of the Ti_2Ni_3Si/NiTi Laves phase alloys, two experimental alloys containing varying Ti, Si contents were designed with a fixed Ni mole fraction of 50%. Chemical compositions of the Ti_2Ni_3Si/NiTi experimental alloys are listed in Table 1. Commercially pure titanium, nickel, and silicon elemental powders with a particle size between 70 μm and 140 μm were selected as the raw materials for preparing Ti_2Ni_3Si/NiTi alloys. The Ti_2Ni_3Si/NiTi alloys were fabricated by the laser melting deposition(LMD) manufacturing process in Ar atmosphere using a newly patented laser melting furnace having a water-cooled copper-mold[19], as schematically illustrated in Fig.1. The well-blended elemental powder mixtures were put into the water-cooled copper-mold and then melted under the direct radiation of a high power laser beam delivered from a 8 kW continuous-wave CO_2 laser. The laser-melt processing parameters were: laser beam output power 2.5 kW, beam diameter 14 mm, laser melting time 30−40 s. Short cylinder-shape ingots with a diameter of approximately 16 mm and a height of approximately 10 mm were produced.

Table 1 Chemical composition of Ti_2Ni_3Si/NiTi alloy (mole fraction, %)

Alloy No.	Ti	Si	Ni
1	39	11	50
2	42	8	50

Metallographic samples and corrosion testing specimens were machined by electric discharging cutting followed by mechanical milling and grinding from the laser-melted short cylinder-like Ti_2Ni_3Si/NiTi Laves phase alloy ingots. Metallographic samples of the Ti_2Ni_3Si/NiTi Laves phase alloy were prepared using standard mechanical polishing procedures and were

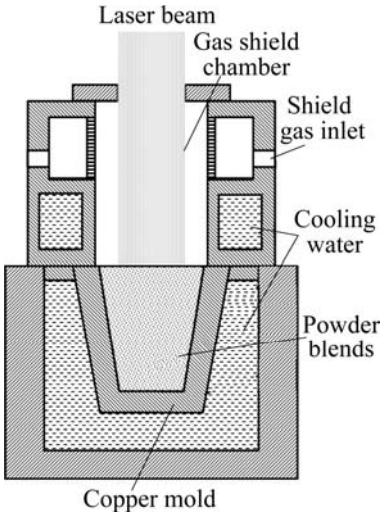

Fig.1 Schematic illustration of water-cooled copper-mold laser melting deposition furnace

chemically etched in HF-HNO_3-H_2O water solution with volume ratio of 1:6:7 at ambient temperature for approximately 10−15 s. The microstructure was characterized by OLYPUS BX51M optical microscope (OM) equipped with a Sisc IAS6.0 image analyzing software and KYKY−2800 scanning electron microscopes(SEM). Powder X-ray diffraction(XRD) was conducted using the Rigaku D/max 2200 pc automatic X-ray diffractometer with Cu target K_α radiation. Chemical compositions of the phase constituents were analyzed by energy dispersive X-ray analysis(EDS) using Noran Ventage DSI spectrometer. Volume fraction of primary dendrites were measured by quantitative metallographic analysis method on high-contrast optical photographs using a commercial contrast-based image analyzing software. Hardness was also measured using an Everone MH−6 semi-automatic Vickers micro-hardness tester with a test load of 4.9 N and a load-dwell time of 15 s.

The mechanical properties of the alloys were studied using a load and displacement sensing indentation technique on the MTS Nano Indenter®XP with a Berkovich diamond tip. Values of effective elastic modulus $E^*=E/(1-\nu^2)$ and hardness were calculated based on the loading/unloading curves measured with a Berkovich indenter using the Oliver–Pharr method[20], where E and ν are the elastic modulus and Poisson ratio of the tested material, respectively. The maximum depth was selected as 2 000 nm and the value of ν was taken as 0.3 during the indentation. The load-depth curves of loading/unloading were recorded automatically and the indentation marks on surface were observed with KYKY−2800 scanning electron microscope(SEM).

The potentio-dynamic anodic polarization tests were carried out on a CHI604 electrochemical corrosion testing apparatus in 1 mol/L NaOH solution in open atmospheric environment at room temperature. All surfaces except one of the corrosion testing samples (10 mm×10 mm×10 mm in size) were sealed with epoxy resin. The only naked surface was then carefully hand-polished with 1000-grit silicon carbide paper and cleaned in distilled water and acetone prior to corrosion testing. The polarization scanning was started at a potential of 0.05 V below the steady open-circuit potential(OCP) with a sweep rate of 5 mV/s to measure the potentio-dynamic anodic polarization curves in reference to a saturated calomel electrode(SCE).

3 Results and discussion

3.1 Chemical composition and microstructure

As shown in Figs.2(a) and (b), alloy 1 with chemical composition of Ni-39Ti-11Si has a uniform hypoeutectic microstructure consisting of the primary dendrite and the interdendritic eutectics due to the rapid heat conduction cooling of water-chilled copper mold. Results of X-ray diffraction (Fig.3) and EDS analysis (primary dendrite: 35.8Ti-44.4Ni-19.8Si and eutectic: 40.5Ti-48.4Ni11.1Si) demonstrate that the primary phase is the Ti_2Ni_3Si Laves phase, while the interdendritic phase is the Ti_2Ni_3Si/NiTi eutectics. Volume fraction of the Ti_2Ni_3Si primary dendrites is approximately 35%. During solidification process, the ternary metal silicide Ti_2Ni_3Si precipitates firstly from the melt as the dendritic primary phase, and then the residual liquid transforms to Ti_2Ni_3Si/NiTi eutectics. On the contrary, the microstructural characteristic of the alloy 2 with chemical composition of Ni-42Ti-8Si is apparently the typical hypereutectic microstructure as shown in Figs.2(c) and (d). Results of X-ray diffraction (Fig.3) and EDS analysis (primary dendrite: 48.4Ti-49.9Ni-1.7Si and eutectic: 38.9Ti-46.4Ni14.7Si) reveal that the dendrites of the alloy 2, other than that of the alloy 1, are NiTi intermetallic compound phase while the eutectics matrix of the alloy 2 consisting of NiTi and Ti_2Ni_3Si is the same as that of the alloy 1. Volume fraction of the NiTi primary dendrites is approximately 40%. During solidification process, the NiTi intermetallic compound phase precipitates from the melt as the dendritic primary phase. Following the precipitation of NiTi, the residual liquid also transforms to Ti_2Ni_3Si/NiTi eutectics.

Obviously, alloy 1 with the chemical composition of Ni-39Ti-11Si is a typical conventional Laves phase intermetallic based alloy having the hypoeutectic microstructure of a hard Laves phase dispersed in a eutectic matrix. Compared with alloy 1, the microstructure of alloy 2 has been changed significantly from hypoeutectic to hypereutectic due to the modification of Si, Ti and Ni contents. Because of the

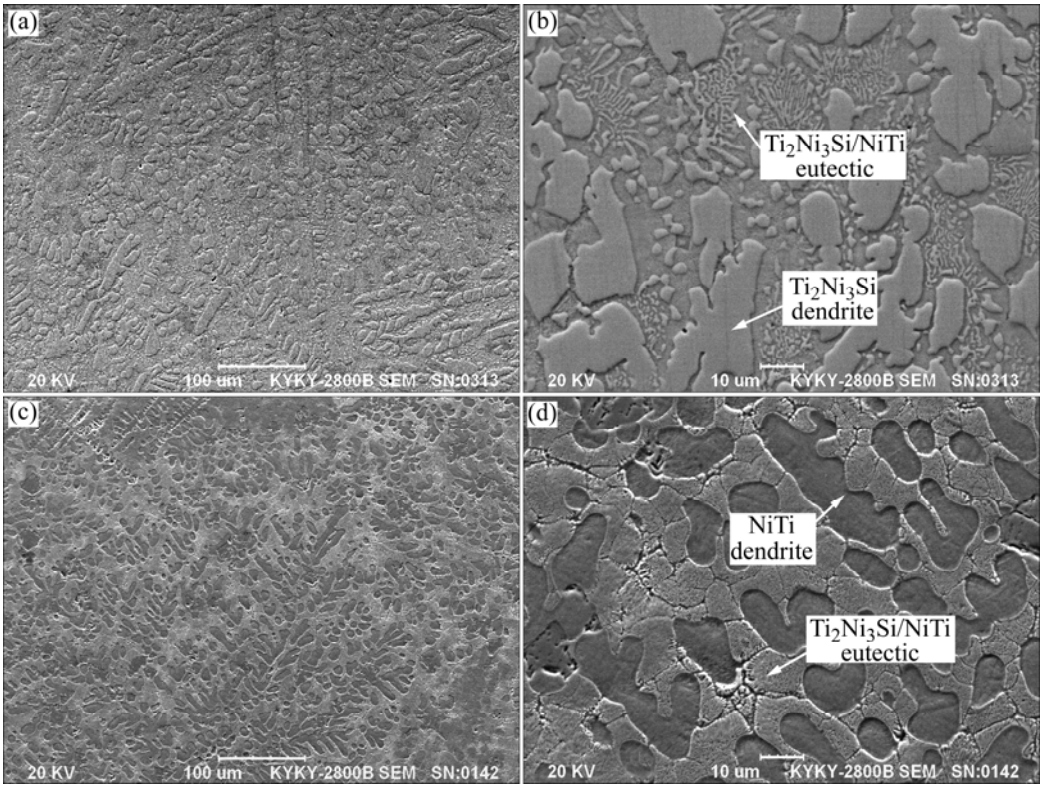

Fig.2 SEM micrographs showing microstructure of alloy 1 low (a), high (b) and alloy 2 low (c), high (d) magnification

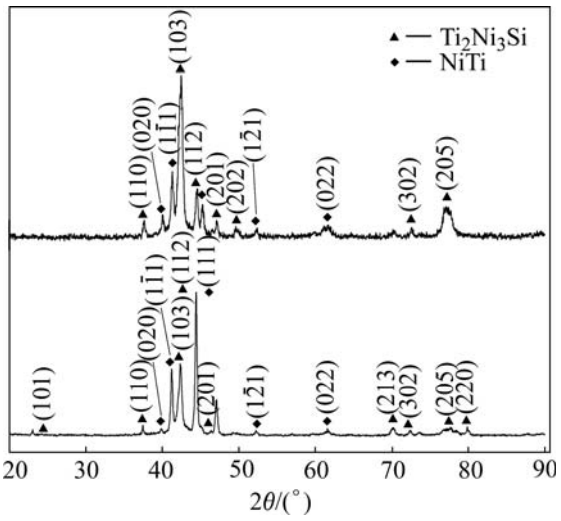

Fig.3 X-ray diffraction patterns of alloys 1 and 2

fixed Ni mole fraction of 50%, the main influence on this transformation is the decrease of Si as well as the increase of Ti content, which changes the solidification process from hypereutectic to hypoeutectic.

3.2 Nanoindentation test

The mechanical behaviors including hardness, elastic modulus, elastic and plastic deformation energy of individual phase in the hypoeutectic alloy 1 and the hypereutectic alloy 2 were investigated using a load and displacement sensing indentation technique on the CSM nano-hardness machine. Fig.4 shows the loading and unloading curves of the nano-indentation on the phase in alloys, As it is known that the area enclosed by the loading curve represents the total deformation energy while that enclosed by the unloading curve reflects the elastic deformation. Therefore, the area between the loading and unloading curves indicates the dissipated energy derived from plastic deformation. Moreover, η_e is defined as the ratio of the elastic deformation energy to the total deformation energy while η_p, being equal to $1-\eta_e$, is the ratio of the plastic deformation energy to the total deformation energy[6−7]. The corresponding mechanical properties such as hardness, elastic modulus and η_e as well as η_p values calculated from the curves are listed in Table 2.

Firstly, comparing the hardness and elastic modulus of the primary phase between the alloys, it is found that the Laves phase Ti_2Ni_3Si of alloy 1 has higher hardness and elastic modulus than the NiTi intermetallic compound of alloy 2. Secondly, comparing the eutectic phase between the alloys, it is found that the eutectic of alloy 1 also has higher hardness and elastic modulus than

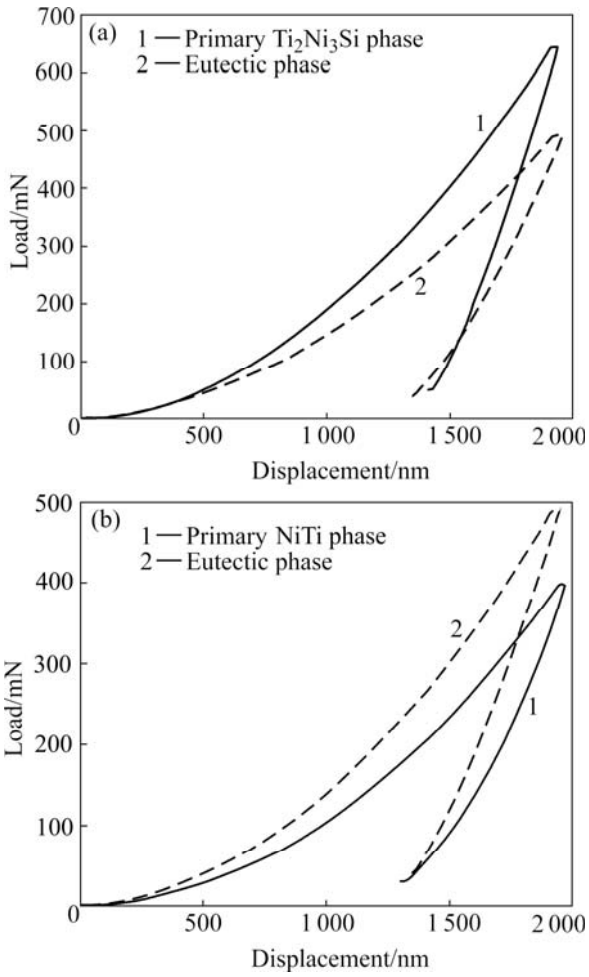

Fig.4 Loading and unloading curves of nanoindentation on alloy 1 (a) and alloy 2 (b)

Table 2 Mechanical properties of tested alloys

Phase	Elastic modulus/GPa	Hardness/ GPa	η_e	η_p
Alloy 1, primary phase	321.832	23.208	0.35	0.65
Alloy 1, eutectic phase	168.033	14.583	0.42	0.58
Alloy 2, primary phase	79.504	6.999	0.44	0.56
Alloy 2, eutectic phase	139.051	11.151	0.43	0.57

that of alloy 2, but the difference in the eutectic phase is much less than that in the primary phase between the two alloys. Thirdly, comparing η_e with η_p values, the primary phase of alloy 1 has a far higher η_p but lower η_e than that of alloy 2. Similarly, the eutectic of alloy 1 also has higher η_p and lower η_e than that of alloy 2. Furthermore, the hardness of alloy 1 and alloy 2 was also tested on an Everone MH−6 semi-automatic Vickers micro-hardness tester. The former has the hardness of HV1117 and the

latter HV703. The results of Vickers hardness are in good agreement with the nano hardness results.

Therefore, the two experiments demonstrate that the overall hardness and elastic modulus of alloy 2 are much lower than that of alloy 1. In the meanwhile, the overall η_e of the alloy 2 is much higher than that of alloy 1 while the overall η_p of the alloy 2 is lower than that of alloy 1. In general, the softer the metallic material, the better the ductility and plasticity[4−7]. However, the results indicate that the ratio of the plastic deformation energy to the total deformation energy of the alloy 2 is lower than that of alloy 1. It may be attributed to the different volume fractions of NiTi intermetallic compound in alloys resulting from the different microstructures. Because of the hyperelasticity of the intermetallic compound NiTi, the capability of the elastic deformation increases dramatically with the increase of the volume fraction of NiTi. Thus, alloy 2 has better elasticity than alloy 1 due to its much larger volume fraction of NiTi, though the alloy 2 is much softer than alloy 1.

3.3 Electrochemical test

Potentio-dynamic anodic polarization curves for the Ti_2Ni_3Si/NiTi alloys measured in 1mol/L NaOH solution open to air at room-temperature are shown in Fig.5. As can be observed, following the active dissolution, both alloy 1 and alloy 2 have a wide steady passive range. The anodic current density of alloy 1 during the passive range is around 10^{-5}−10^{-4}A/cm^2, a little higher than that of alloy 2. The anodic current density of alloys rises quickly at potential of about 0.4 and 0.5V (vs SCE), respectively, which is suggested to be due to transpassive dissolution of alloys. The results indicate that both alloy 1 and alloy 2 exhibit excellent corrosion resistance in 1 mol/L NaOH solution under the anodic polarization test, characterized by their wide passivation region and fairly low passive anodic current density, although the microstructures of two alloys are quite different. The high corrosion resistance of alloys is supposed to be due to the synergistic effect of constituent elements Ti, Ni and Si. It is known that Ti, Ni and Si are all strong passive elements in aggressive environments. A continuous, stable and extremely protective passive oxide film TiO_2 can be easily and spontaneously formed because of the high affinity for oxygen of titanium in all kinds of natural environments especially in oxidizing acids while a dense protective passive film $Ni(OH)_2$ can be formed and exist stably on the surface of alloy containing nickel content in all neutral and alkaline solutions[21−22].

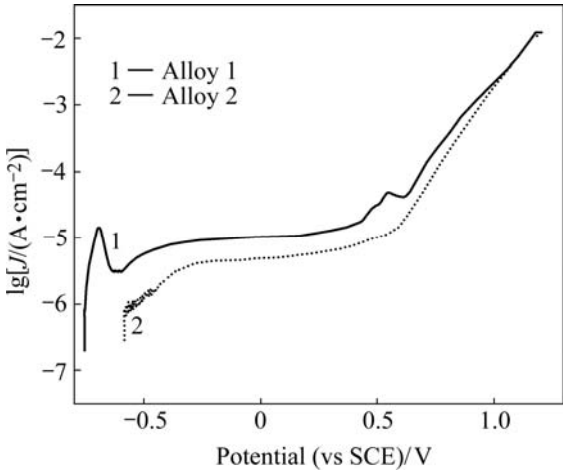

Fig.5 Potentio-dynamic anodic polarization curves of alloy 1 and alloy 2 in 1mol/L NaOH solution

4 Conclusions

1) Two Ti_2Ni_3Si/NiTi Laves phase alloys were fabricated by laser melting deposition process. Because of the modification of Si, Ti contents, the hypereutectic alloy 1 with chemical composition of Ni-39Ti-11Si consists of a hard intermetallic Laves phase dispersed in a matrix of Ti_2Ni_3Si/NiTi eutectic while the hypoeutectic alloy 2 with chemical composition of Ni-42Ti-8Si has a dual-phase microstructure consisting of NiTi primary dendrites uniformly distributed in Ti_2Ni_3Si/NiTi eutectic.

2) The alloy 2 is much softer than alloy 1 evidenced by the hardness and elastic modulus of the alloys while the elasticity (η_e value) of alloy 2 increases greatly compared with that of alloy 1. These differences are attributed to the different volume fractions of NiTi originating from the different concentrations of Ti and Si.

3) Both alloy 1 and alloy 2 exhibit excellent corrosion properties in NaOH solution characterized by their similar potentio-dynamic anodic polarization curves. This is ascribed to the formation of a protective passive film on both the surface of alloys.

Acknowledgement

The authors would like to thank Mr ZHANG Ling-yun and Ms YU Rong-li for their invaluable assistance during the laser melting deposition and the metallographic experiments.

References

[1] LIU C T, STRINGER J, MUNDY J N. Ordered intermetallic alloy: An assessment [J]. Intermetallics, 1999, 5: 579−596.

[2] LIU C T, ZHU J H, BRADY M P, MCKAMEY C G, PIKE L M. Physical metallurgy and mechanical properties of transition-metal Laves phase alloys [J]. Intermetallics, 2000, 8: 1119−1129.

[3] SAUTHOFF G. Multiphase intermetallic alloys for structural applications [J]. Intermetallics, 2000, 8: 1101−1109.

[4] LIN W C, CHEN C. Characteristics of thin surface layers of

cobalt-based alloys deposited by laser cladding [J]. Surface and Coatings Technology, 2006, 200: 4557−4563.

[5] YAO M X, WU J B C, YICK S. High temperature wear and corrosion resistance of a Laves phase strengthened Co-Mo-Cr-Si alloy [J]. Mater Sci Eng A, 2006, 453/456: 78−83.

[6] LIU R, XU W, YAO M X. A newly developed Tribaloy alloy with increased ductility [J]. Scripta Materialia, 2005, 53: 1351−1355.

[7] YAO M X, WU J B C, LIU R. Microstructural characteristics and corrosion resistance in molten Zn-Al bath of Co-Mo-Cr-Si alloys [J]. Mater Sci Eng A, 2005, 407: 299−305.

[8] WANG H M, LUAN D Y, ZHANG L Y. Microstructure and wear resistance of laser melted W/W_2Ni_3Si metal silicides matrix in situ composites [J]. Scripta Materialia, 2003, 48: 1179−1184.

[9] LU X D, WANG H M. High-temperature sliding wear behaviors of laser clad Mo_2Ni_3Si/NiSi metal silicide composite coatings [J]. Applied Surface Science, 2003, 214: 190−195.

[10] LIU Y, WANG H M. Microstructure and high-temperature sliding wear property of Co_{ss}/Co_3Mo_2Si metal silicide alloys [J]. Mater Sci Eng A, 2005, 396: 240−250.

[11] MIYAZAKI S, IMAI T, IGO Y, OTSUKA K. Effect of cyclic deformation on the pseudoelasticity characteristics of Ti-Ni alloys [J]. Metallurgical Transactions, 1986, A17: 115−120.

[12] MIYAZAKI S, OTSUKA K, SUZUKI Y. Transformation pseudoelasticity and deformation behavior in a Ti-50.6at%Ni alloy [J]. Scripta Metallurgica, 1981, 15: 287−292.

[13] LI D Y. Wear behaviour of TiNi shape memory alloys [J]. Scripta Materialia, 1996, 34: 195−200.

[14] LI D Y. Development of novel wear-resistant materials: TiNi-based pseudoelastic tribomaterials [J]. Materials and Design, 2000, 21: 551−555.

[15] CHENGA F T, SHI P, PANG G K H. Microstructural characterization of oxide film formed on NiTi by anodization in acetic acid [J]. Journal of Alloys and Compounds, 2007, 438: 238−242.

[16] RONDELLI G, VICENTINI B, CIGADA A. The corrosion behaviour of nickel titanium shape memory alloys [J]. Corrosion Science, 1990, 30: 805−812.

[17] WANG H M, CAO F, CAI L X, TANG H B, YU R L, ZHANG L Y. Microstructure and tribological properties of laser clad Ti_2Ni_3Si/NiTi intermetallic coatings [J]. Acta Materialia, 2003, 51: 6319−6327.

[18] WANG Y, WANG H M. Wear resistance of laser clad Ti_2Ni_3Si reinforced intermetallic composite coatings on titanium alloy [J]. Applied Surface Science, 2004, 229: 81−86.

[19] WANG H M, ZHANG L Y. Laser smelting furnace with water cooled copper mould and method for smelting ingot [P]. CN02121496.4, 2002−06−26. (in Chinese)

[20] OLIVER W C, PHARR G M. Improved technique for determining hardness and elastic modulus using load and displacement sensing indentation experiments [J]. Journal of Materials Research, 1992, 7: 1564−1580.

[21] HUANGA Y Z, BLACKWOOD D J. Characterisation of titanium oxide film grown in 0.9% NaCl at different sweep rates [J]. Electrochimica Acta, 2005, 51: 1099−1107.

[22] ALVES H, FERREIRA M G S, KOSTER U. Corrosion behavior of nanocrystalline $(Ni_{70}Mo_{30})_{90}B_{10}$ alloys in 0.8M KOH solution [J]. Corrosion Science, 2003, 45: 1833−1845.

(Edited by LI Xiang-qun)